이학석사 학위논문

# 간단한 상 변화를 통한 다양한 형태의 $Fe_3O_4$ 나노 입자 합성 및 형태 의존적 자기 특성의 이해

# Synthesis of various magnetite nanoparticles through the simple phase transformation and their shape-dependent magnetic properties

2013 년 2 월

서울대학교 대학원
화학부 무기화학
최 제 남

# 간단한 상 변화를 통한 다양한 형태의 $Fe_3O_4$ 나노 입자 합성 및 형태 의존적 자기 특성의 이해

# Synthesis of various magnetite nanoparticles through the simple phase transformation and their shape-dependent magnetic properties

지도 교수 이 진 규

이 논문을 이학석사 학위논문으로 제출함

2013 년 2 월

서울대학교 대학원

화학부 무기화학

최 제 남

최제남의 이학석사 학위논문을 인준함

2012 년 12 월

위 원 장 남 좌 민 (인)

부위원장 이 진 규 (인)

위 원 손 병 혁 (인)

# Abstract

## Synthesis of various magnetite nanoparticles through the simple phase transformation and their shape-dependent magnetic properties

Jenam Choi

Department of Chemistry

The Graduate School

Seoul National University

Shape-controlled synthesis of iron oxide nanoparticles had been successfully carried out through the simple phase transformation via polyol process using akaganeite (β-FeOOH) as a single precursor material. Different shapes of iron oxide nanoparticles including solid spheres, solid rods, and hollow rods could be obtained by either adding appropriate amount of sodium acetate (NaOAc) or the anion exchange of β-FeOOH. The possible mechanism for formation of $Fe_3O_4$ with different shapes was proposed. The NaOAc could make it possible to retain the rod shape of precursor materials (β-FeOOH) during the phase transformation by coordinating the surface and controlling basic pH to slow down dissolution-recrystallization mechanism. We also proposed that chloride ions in β-FeOOH structure play a key role in the formation of hollow structure. The shape-dependent magnetic properties were investigated with magnetic property measurement system at 300K. All iron oxide nanoparticles exhibited ferromagnetic behavior with

different value of saturation magnetization ($M_s$) and coercivity ($H_c$) which highly depended on the shape of the nanoparticles due to their different grain size, spin disorder, shape and surface anisotropy. It would be systematic studies of shape-dependent magnetic properties, especially for comparison between hollow rods and solid rods, because of their comparable structural size and average grain size and negligible effect of other parameters such as surfactant that could affect crystallinity and crystal defects of nanoparticles.

**Keywords :** Akaganeite (β-FeOOH), Magnetite ($Fe_3O_4$), Shape-controlled synthesis, Phase transformation, Shape-dependent properties

**Student Number :** 2011-20309

# Table of contents

**Abstract** ..... **1**

**List of Figures and Table** ..... **4**

**Introduction** ..... **6**

**Experimental Section** ..... **8**

**Result and Discussion** ..... **12**

**Conclusion** ..... **26**

**Reference** ..... **28**

**Abstract (in Korean)** ..... **33**

**Acknowledgements (in Korean)** ..... **35**

# List of Figures and Table

**Figure 1.** Schematic illustration of the formation process of magnetite ($Fe_3O_4$) in various shapes through the phase transformation reaction from akaganeite (β-FeOOH)

**Figure 2.** TEM images of (a) Cl-FeOOH, (b) solid $Fe_3O_4$ nanospheres obtained from (a), (c) hollow $Fe_3O_4$ nanorods obtained from (a), (e) OH-FeOOH, (f) solid $Fe_3O_4$ nanospheres obtained from (e), (g) solid $Fe_3O_4$ nanorods obtained from (e). Plot of the relative amount of each element (O and Fe) as a functions of position for the (d) hollow $Fe_3O_4$ and (h) solid $Fe_3O_4$ nanorods

**Figure 3.** XRD patterns of synthesized (a) Cl-FeOOH (b) OH-FeOOH after anion exchange, (c) solid $Fe_3O_4$ nanospheres obtained from (a), (d) hollow $Fe_3O_4$ nanorods obtained from (a), (e) solid $Fe_3O_4$ nanorods obtained from (b), (f) solid $Fe_3O_4$ nanorods obtained from (b)

**Figure 4.** TEM images of the products obtained at various NaOAc amount; (a) 5mmol, (b) 15mmol (optimized condition), (c) 45 mmol, and (d) XRD patterns of product shown in (a), (b), and (c) respectively.

**Figure 5.** TEM images of the products obtained with different salts; (a) 15 mmol NaCl, (b) 15 mmol NaOH, and (c) the mixture of NaOH (10 mmol) and NaAc (15 mmol)

**Figure 6.** Room temperature magnetic hysteresis curves for (a) the solid $Fe_3O_4$ nanospheres, (b) the solid $Fe_3O_4$ nanorods, (c) the hollow $Fe_3O_4$ nanorods. Inset shows the detail in the low field region.

**Figure 7.** $N_2$ adsorption and desorption isothermals and pore size distribution of (a) the hollow $Fe_3O_4$ nanorods, (b) the solid $Fe_3O_4$ nanorods

**Figure 8.** $T_1$ and $T_2$ relaxation rate ($1/T_1$, $1/T_2$) plotted against the Fe concentration for (a) hollow $Fe_3O_4$ and (b) solid $Fe_3O_4$ nanorods (0.47 T, 37 ℃)

**Table 1.** $Cl^-$ ions content in β-FeOOH measured by EDS

**Table 2.** $T_1$ and $T_2$ relaxivities of hollow and solid $Fe_3O_4$ nanorods

# Introduction

In the past decade, nanostructured magnetite($Fe_3O_4$) have been considered attractive materials due to their intrinsic magnetic features combined with the high surface area to volume ratio and potential applications in magnetic storage media, magnetic separation, contrast agents in magnetic resonance imaging (MRI), catalysts, drug delivery and hyperthermia etc.[1-8] Thus there have been many efforts to develop the synthetic method for the magnetite nanoparticles such as co-precipitation, thermal decomposition, hydrothermal and solvothermal synthesis etc.[9-12] Recently a polyol method has attracted researchers' attention for its capabilities in synthesizing magnetite with hydrophilic surfaces and high crystallinity which result from relatively higher reaction temperature.[13] Moreover, phase transformation from a certain oxyhydroxide (FeOOH) or iron oxide ($Fe_2O_3$) to magnetite ($Fe_3O_4$) may be also possible due to reducing ability of polyol in this method. However, there are few reports about phase transformation through the polyol method. Some groups just reported the phase transformation for magnetite by using reducing agent such as hydrazine, sodium borohydride etc. via solution process. [14-16]

There has also been increasing attention paid to the design and synthesis of magnetic materials with controlled size and shape such as nanospheres, nanorods, nanotubes, nanowires and hollow structures etc.[6, 12, 17-19] Magnetic properties of materials are usually very sensitive to its shape due to the dominating role of

anisotropy in magnetism. For that reason, it is desirable to develop strategies for shape-controlled synthesis of magnetite nanoparticles. However, most previous reports focused on the synthesis of $Fe_3O_4$ nanoparticles without investigation of shape-dependent magnetic properties. In addition, the sophisticated interpretation of the shape-dependent magnetic properties was difficult, because it is difficult to synthesize the shape-controlled nanoparticles with comparable size under the same experimental condition such as temperature, solvent, precursor, reducing agent, surfactants and so on. In general, the magnetic properties vary depending on the synthetic condition which may affect crystallinity and crystal defects of generated nanoparticles,[20-22] even though they have similar size and shape.

Herein, we report a simple polyol method for synthesis of shape-controlled magnetite nanostructure, i.e. solid nanospheres, solid nanorods, and hollow nanorods through the phase transformation from a single precursor material. The synthetic method presented here is attractive due to simple and economical procedure without employing surfactants or reducing agents, which enable us to scale up easily. We expect that it is possible to understand more accurately the shape-dependent magnetic properties through our new synthetic method of the phase transformation from a same precursor material by minimizing effects from experimental parameters as mentioned above.

Furthermore, we carried out MRI experiments with the hollow and solid $Fe_3O_4$ nanorods to confirm their potential ability as MRI contrast agents.

# Experimental Section

## Chemicals

$FeCl_3 \cdot 6H_2O$ (>97%, Simga-Aldrich), sodium acetate anhydrous (>98.5%, Samchun Chemicals), and ethylene glycol (EG, >99.5%, Samchun Chemicals) were obtained from commercial sources and used as received.

## Preparation of akaganeite (β-FeOOH or $Fe^{3+}O(OH,Cl)$)

Rod-shaped akaganeite was prepared from hydrolysis of $FeCl_3$ solution by slightly modifying the reported method in literature.[23] 5.4 g $FeCl_3 \cdot 6H_2O$ was dissolved in 500 mL deionized water in a 1 L two-neck round bottom flask at room temperature. The solution was heated at 80 ℃ and kept for 24 h with mechanical stirring. The solution was then allowed to cool down to room temperature and centrifuged to obtain yellowish-brown precipitate. The precipitate was then washed several times with deionized water to remove unreacted iron precursor. The akaganeite (Cl-FeOOH) nanoparticles were stored in as aqueous solution as precursor materials for phase transformation reactions.

## Synthesis of magnetite ($Fe_3O_4$) with different shapes : Solid nanospheres, Hollow nanorods, Solid nanorods

Solid $Fe_3O_4$ nanospheres were prepared by adding 5 mmol Cl-FeOOH into 500 mL of ethylene glycol in 1 L two-neck round bottom flask. The mixture was refluxed for 6 h with mechanical stirring.

Hollow $Fe_3O_4$ nanorods were prepared by adding 5 mmol Cl-FeOOH into 500 mL ethylene glycol containing 15 mmol sodium acetate (NaOAc) in 1 L two-neck round bottom flask. The mixture solution was refluxed for 24 h with mechanical stirring.

On the other hand, the preparation of solid $Fe_3O_4$ nanorods was similar to that of hollow $Fe_3O_4$ nanorods except for the use of OH-FeOOH instead of Cl-FeOOH as precursor materials. OH-FeOOH was easily prepared from Cl-FeOOH by anion exchange as reported; Cl-FeOOH has the three-dimensional tunnel structure containing chloride ions, which can be substituted with hydroxide ions through the anion exchange reaction.[24, 25] Briefly, as-prepared 5 mmol of Cl-FeOOH was added to 100 mL of 0.5 M NaOH solution and the solution was heated at 55℃ for 3 h with magnetic stirring. The anion-exchanged akaganeite (OH-akaganetie) was collected by centrifugation and washed several times with deionized water. Mohr titration method[26] and EDS were used to determine the amount of chloride ions released from the Cl-FeOOH in the anion exchange reaction. All products (solid $Fe_3O_4$

nanospheres, hollow $Fe_3O_4$ nanorods, solid $Fe_3O_4$ nanorods) obtained from phase transformation reaction were collected using centrifugation, washed with ethanol several times and stored in ethanol for characterization.

## Characterization

The size and morphology of the synthesized products were investigated with Transmission Electron Microscope (Hitachi-7600, Hitachi, 100 kV and JEM-2100, JEOL, 200 kV). High resolution (HR) TEM images and EDS line scanning images were obtained by a Tecnai F20 with an accelerating voltage of 200 kV. Crystal structure and phase analysis of the products were performed by X-ray diffractometer (M18XHF-SRA, MAC Science Co., Cu-$K_\alpha$ $\lambda$=0.15409 nm). The nitrogen absorption and desorption isothermals were measured by the Brunauer-Emmett-Teller (BET) method with surface area and pore characterization system (ASAP 2020, Micromeritics). Magnetic properties were investigated with magnetic property measurement system (MPMS-7, Quantum Design) at 300K by cycling the field between -7 kOe and 7 kOe.

## MRI relaxation time measurement

$T_1$ and $T_2$ relaxation times of hollow and solid Fe3O4 nanorods with various concentrations were measured using Minispec spectroscopy (MQ20 NMR Analyzer, 37 ℃, 0.47 T). We derived relaxivities based on the molar concentration of Fe atoms measured by ICP-AES.

It was well known that the dispersibility of nanoparticles were very important for their application in biomedicine. For water dispersibility of the synthesized $Fe_3O_4$ nanoparticles (hollow rods and solid rods), they were surface-modified with excess PAA (poly acrylic acid 35 wt. % solution in water, $M_w$: 100 K). 20 mg of $Fe_3O_4$ in 4 mL of water and 10 mL of PAA aqueous solution (20 mg/mL) were mixed and followed by stirring for 1 h. After centrifugation and washing with water 2 times, 2~3 drops of ammonia solution (28~30 %) was added to $Fe_3O_4$ redispersed in water.

# Result and discussion

Magnetite ($Fe_3O_4$) nanoparticles with different shapes were synthesized through the simple phase transformation with akaganeite (β-FeOOH) as single precursor materials. This method is modified existing polyol method using ethylene glycol (EG) which acts as not only solvent with high boiling point but also reducing agent.[6, 27] The overall scheme of synthesis process was shown in **Fig. 1**. The shape of $Fe_3O_4$ nanoparticles was easily varied from solid nanospheres, hollow nanorods and solid nanorods by adding appropriate amount of sodium acetate (NaOAc) as well as exchanging the anion of Cl-FeOOH to form OH-FeOOH.

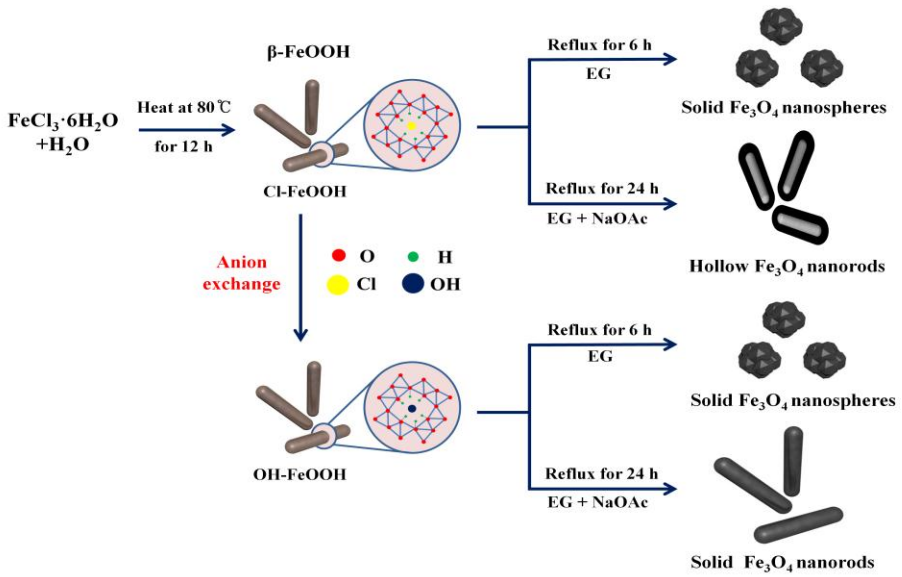


**Figure 1.** Schematic illustration of the formation process of magnetite ($Fe_3O_4$) in various shapes through the phase transformation reaction from akaganeite (β-FeOOH)

Cl-FeOOH was synthesized from hydrolysis of iron(Ⅲ) chloride aqueous solution.[23] TEM image of the Cl-FeOOH shown in **Fig. 2 (a)** revealed rod-shaped nanoparticles with diameter of ~50 nm and length of ~180 nm even though a size distribution was not narrow. The peaks in the XRD pattern (**Fig. 3 (a)**) were matched well with the reported akaganeite structure,[14] confirming the purity of product without containing other crystalline products such as hematite ($\alpha$-$Fe_2O_3$).

The solid $Fe_3O_4$ nanospheres (**Fig. 2 (b), (f)**) were formed by refluxing the dispersed solution of β-FeOOH (either Cl-FeOOH or OH-FeOOH) in ethylene glycol. Phase transformation took place from β-FeOOH to $Fe_3O_4$ through the partial reduction ($Fe^{3+} \rightarrow Fe^{2+}$) by EG without adding any reducing agent. During the phase transformation of the β-FeOOH via solution process un bulk states, dissolution-recrystallization mechanism has been widely known.[15, 16, 28] Reductive reaction environment could also assist the dissolution of β-FeOOH which led the structural bonds between Fe atoms in β-FeOOH to be weaken by reduction of $Fe^{3+}$ to $Fe^{2+}$. Dissolved ferrous ($Fe^{2+}$) ions into solution brought about more rapid dissolution of Fe atoms by the catalytic action as reported in the literature.[29,30] Dissolved $Fe^{2+}$ ions would interact with surface groups of β-FeOOH and following nucleation of magnetite would take place.[31] According to this dissolution-recrystallization

mechanism, $Fe_3O_4$ nanoparticles with different shape in the size of 50~80 nm nanosphere could be obtained within 6 h from β-FeOOH having nanorod shape.

On the other hand, the $Fe_3O_4$ nanoparticles with rod shape (**Fig. 2 (c), (g)**) were obtained when NaOAc was added into the mixture of β-FeOOH (Cl-FeOOH or OH-FeOOH) and EG, which had comparable size and shape with those of β-FeOOH. In those cases, the reaction time to complete phase transformation was about four times longer than the case without adding NaOAc. From this result, it was assumed that NaOAc was critical to maintain the rod shape during phase transformation by slowing down the dissolution rate of $Fe^{2+}$ from β-FeOOH. Since the dissolution rate was slow, the whole β-FeOOH nanorods could be converted into $Fe_3O_4$ nanorods through the direct reduction and migration[16] which might take longer time than dissolution-recrystallization reaction.

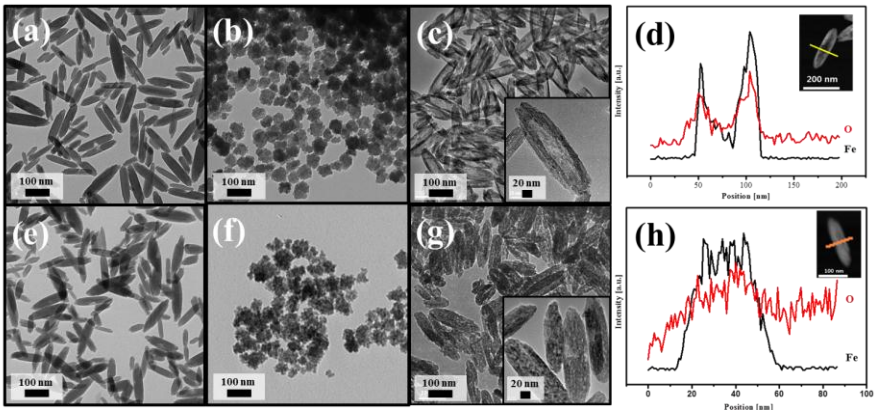


**Figure 2**. TEM images of (a) Cl-FeOOH, (b) solid $Fe_3O_4$ nanospheres obtained from (a), (c) hollow $Fe_3O_4$ nanorods obtained from (a), (e) OH-FeOOH, (f) solid $Fe_3O_4$ nanospheres obtained from (e), (g) solid $Fe_3O_4$ nanorods obtained from (e). Plot of the relative amount of each element (O and Fe) as a functions of position for the (d) hollow $Fe_3O_4$ and (h) solid $Fe_3O_4$ nanorods

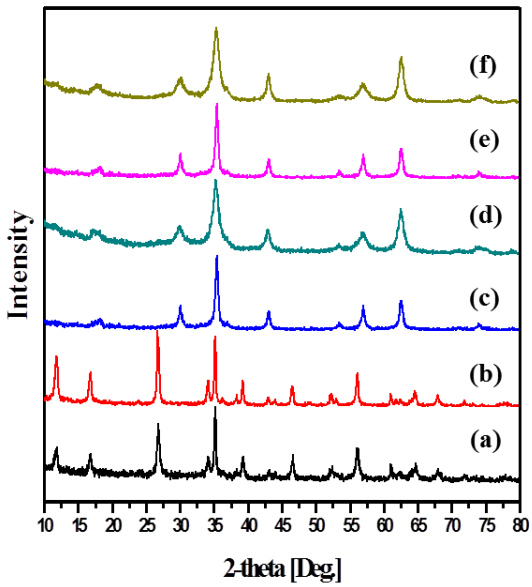


**Figure 3.** XRD patterns of synthesized (a) Cl-FeOOH (b) OH-FeOOH after anion exchange, (c) solid $Fe_3O_4$ nanospheres obtained from (a), (d) hollow $Fe_3O_4$ nanorods obtained from (a), (e) solid $Fe_3O_4$ nanorods obtained from (b), (f) solid $Fe_3O_4$ nanorods obtained from (b)

When different amount of NaOAc was added during the phase transformation of Cl-FeOOH in EG, incomplete phase transformation and irregular shapes were observed as shown in **Figure 4**. With smaller amount of NaOAc (5 mmol, 1/3 of optimized amount), the shape of nanoparticles wasn't maintained well although the phase transformation from β-FeOOH to $Fe_3O_4$ was complete. (**Fig 4 (a), (d)**) With larger amount of NaOAc (45 mmol, 3 times of optimized amount), however, the phase transformation from β-FeOOH to $Fe_3O_4$ was incomplete although the shape of nanoparticles was maintained after 24 h. (**Fig 4 (c), (d)**) This result revealed that our assumption was reasonable.

The effect of pH and salt which resulted in different shape of product was also investigated. The solid nanospheres (**Fig 5 (a)**) were obtained with NaCl which didn't make a change in the pH of solution. Whereas the shape of nanoparticles obtained with NaOH which increased the pH of solution was similar to those obtained with NaOAc and they seemed to be more irregular. (**Fig 5 (b)**) Without adding NaOH, the pH of solution was 2.6±0.3, because β-FeOOH was synthesized in acidic condition. At low pH, the proton adsorption weakened the Fe-O bond probably by polarizing it and promoted detachment of Fe from the β-FeOOH as proposed in the literature.[31, 32] It would be noticeable in reductive condition of high temperature. Even though NaOH was more basic than NaOAc, coordination ability of acetate anions seemed to affect the maintence of nanoparticles shape. When β-FeOOH solution was treated with mixed salt of NaOAc and NaOH, products showed more regular shape, although the pH of solution was almost same to those

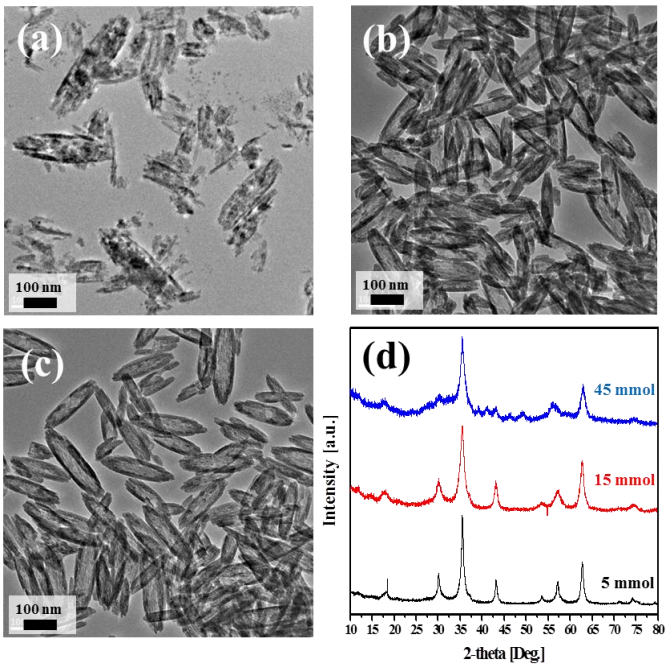


**Figure 4.** TEM images of the products obtained at various NaOAc amount; (a) 5mmol, (b) 15mmol (optimized condition), (c) 45 mmol, and (d) XRD patterns of products shown in (a), (b), and (c) respectively.

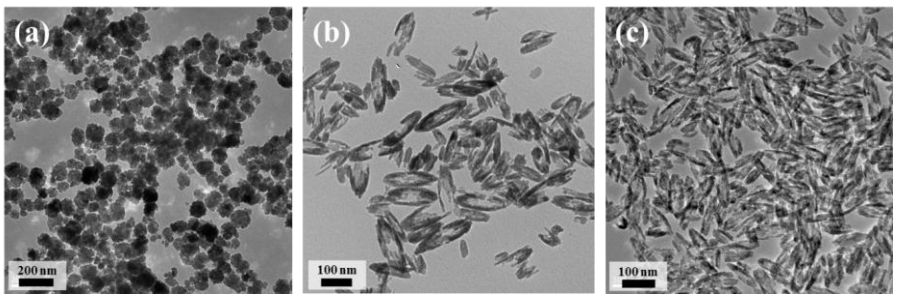


**Figure 5.** TEM images of the products obtained with different salts; (a) 15 mmol NaCl, (b) 15 mmol NaOH, (c) the mixture of NaOH (10 mmol) and NaOAc (15 mmol)

when using only NaOH (**Fig. 5 (c)**). The carboxylate groups in acetate anions have strong interaction with $Fe^{3+}$ in surface of FeOOH[33], which could help the shape maintain. In summary, NaOAc would retain the rod shape of precursor (β-FeOOH) during phase transformation by providing the basic pH which lead to decrease the dissolution rate of β-FeOOH and the coordination to surface of β-FeOOH which could assist the shape maintenance.

On the other hand, formation of hollow structure was induced by chloride ions in Cl-FeOOH structure. It was known that Cl-FeOOH has the three-dimensional tunnel structure[34] which contains both chloride ions and proton ions. Because Cl-FeOOH was synthesized in an acidic environment, Cl-FeOOH would uptake protons from solution as shown in the following equation[35]:

$$FeOOH\ (s) + x\ H^{+}(aq) \rightarrow FeOOH_{1+x}^{\ x+}$$

The tunnels in the Cl-FeOOH structure were considered to be stabilized by the chloride anions balancing stoichiometrically the extra protonation.[24, 25, 34] Chloride ions captured in tunnel structure of Cl-FeOOH were easily removed through anion exchange with hydroxide ions. The amount of chloride ions released from Cl-FeOOH was determined by Mohr-titration as $4.52 \times 10^{-4}$ mol (9 mol %). Moreover, the amount of chloride ions left in OH-FeOOH after anion exchange was compared with Cl-FeOOH by EDS, showing that 77% chloride ions were replaced. (**Table. 1**)

**Table 1 $Cl^-$ ions content in β-FeOOH measured by EDS**

| Akaganeite | Cl content (% mass) |
|---|---|
| **Before anion exchange** | **4.9 ± 0.5** |
| **After anion exchange** | **1.1 ± 0.1** |

Although there was no significant changes of crystal structure after anion exchange (**Fig.3 (b)**), OH-FeOOH showed obvious difference compared to Cl-FeOOH in shape of nanoparticles after phase transformation with NaOAc, producing solid nanorods instead of hollow nanorods. Therfore, chloride ions in Cl-FeOOH structure should play the crucial role in the formation of hollow structure, even though details about the formation mechanism of hollow structure by chloride ions was not clear and further investigation would be necessary. It is the template-free method, so this proposed method is very simple and economical compared to previously reported procedures for preparing the hollow structure.[23, 36]

As mentioned above, the hollow and solid nanorods nanoparticles were obtained respectively depending on either Cl-FeOOH or OH-FeOOH as precursor materials. But the solid nanospheres nanoparticles were obtained without adding NaOAc regardless of using Cl-FeOOH or OH-FeOOH. It could be because the chloride ions in Cl-FeOOH structure were released to solution by dissolution and subsequently the

recrystallization occurred except for chloride ions which were not unnecessary for $Fe_3O_4$.

The magnetic properties of $Fe_3O_4$ nanoparticles with different morphologies were investigated with magnetic property measurement system at 300K in the applied field from -7 kOe to 7 kOe. The magnetic hysteresis curves of the solid $Fe_3O_4$ nanospheres, solid $Fe_3O_4$ nanorods and hollow $Fe_3O_4$ nanorods are shown in **Fig.6**. It can be seen that all $Fe_3O_4$ nanoparticles showed ferromagnetic behavior, but values of saturation magnetization ($M_s$) and coercivity ($H_c$) were different depending on the shape of the nanoparticles as expected.

The saturation magnetization ($M_s$) values were decreased in order of solid $Fe_3O_4$ nanospheres (94.1 emu/g), solid $Fe_3O_4$ nanorods (65.6 emu/g) and hollow $Fe_3O_4$ nanorods (53.0 emu/g). The solid $Fe_3O_4$ nanospheres have the highest value of $M_s$ which is similar to the known value for bulk magnetite ($M_s$=92 emu/g), confirming that produced magnetite nanospheres in the size of 50~80 nm with average grin size 14.8 nm (calculated respectively according to the Debye-Sherrer equation ($0.9\lambda/\beta\cos\theta$)[37] have strong magnetic properties. Average gain size for nanorods were calculated as smaller as 7.0 nm and 6.4 nm for solid $Fe_3O_4$ nanorods and hollow $Fe_3O_4$ nanorods, respectively. It is well matched with the known trend that the bigger grain size is, the higher value of saturation magnetization is.[38] On the other hand, the saturation magnetization value of solid $Fe_3O_4$ nanorods was higher than that of hollow $Fe_3O_4$ nanorods, although both had similar average nanorod size and grain s

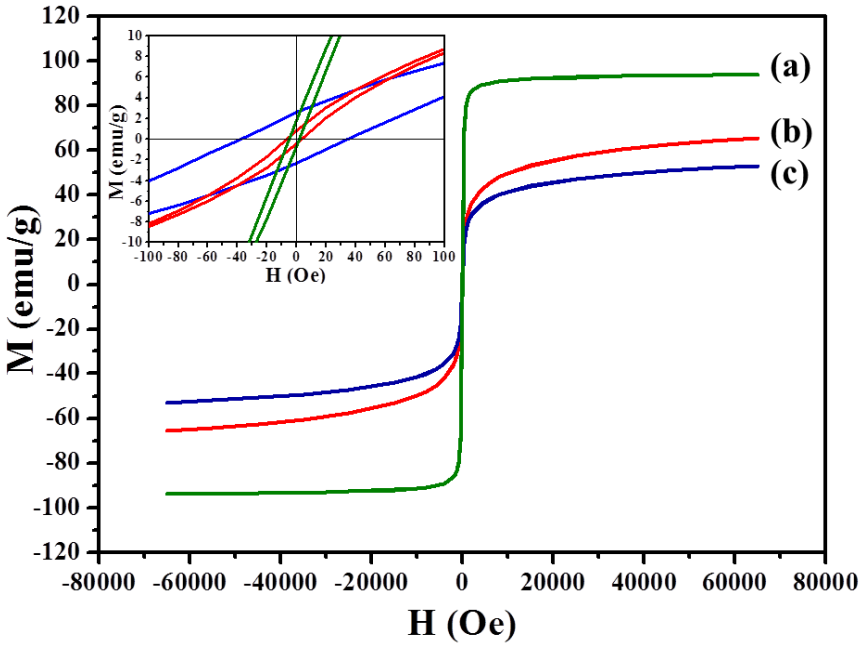


**Figure 6.** Room temperature magnetic hysteresis curves for (a) the solid $Fe_3O_4$ nanospheres, (b) the solid $Fe_3O_4$ nanorods, (c) the hollow $Fe_3O_4$ nanorods. Inset shows the detail in the low field region.

size. It could be explained by spin-canting effect, which resulted from the lack of full alignment of the spins in surface atoms, and was known to be lead the low magnetization.[39]

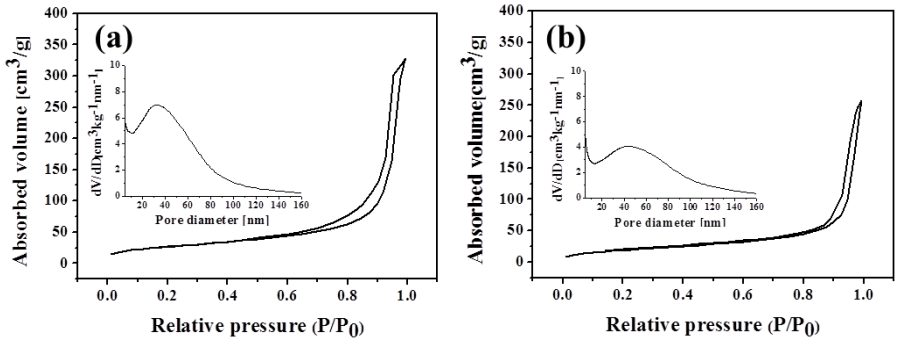


**Figure 7.** $N_2$ adsorption and desorption isothermals and pore size distribution of (a) the hollow $Fe_3O_4$ nanorods, (b) the solid $Fe_3O_4$ nanorods

The measured Brunauer-Emmett-Teller (BET) surface area of hollow $Fe_3O_4$ nanorods and solid $Fe_3O_4$ nanorods were 91.6 $m^2/g$ and 68.9 $m^2/g$ respectively **(Fig.7),** which can be a direct evidence for smaller $M_s$ value of hollow $Fe_3O_4$ nanorods by spin canting effect.

As for coercive force ($H_c$), it was decreased in order of hollow $Fe_3O_4$ nanorods (37.8 Oe), solid $Fe_3O_4$ nanorods (6.5 Oe) and solid $Fe_3O_4$ nanospheres (5 Oe), which was interestingly in the reverse order of $M_s$ values. According to Stoner-Wohlfarth theory, the coercive force of nanoparticles is given by the following equation:[37]

$$H_c = \frac{2K}{\mu_0 M_s}$$

where $\mu_0$ is the vacuum permeability, $M_s$ is the saturation magnetization, and K is the anisotropy constant, which can be influenced by several intrinsic factors of the nanoparticles such as magnetocrystalline, surface and shape.[40]

The solid $Fe_3O_4$ nanospheres had the smallest $H_c$, due to the highest $M_s$ and their spherical shape which resulted in almost zero of shape anisotropy. On the other hand, the hollow $Fe_3O_4$ nanorods had the largest $H_c$. ; having the largest surface area to induced the high surface anisotropy, and smallest $M_s$ value due to spin disorder. Moreover, the rod shape which had high shape anisotropy could lead to larger K and $H_c$.

The $Fe_3O_4$ nanoparticles with different shapes have demonstrated the distinctly different saturation magnetization and coercivity. It was attributed by their different average grain size, spin disorder, shape and surface anisotropy. It would be systematic studies of shape-dependent magnetic properties, especially for comparison between hollow rods and solid rods. It was because they had comparable structure size and average grain size. Furthermore the effect of other experimental parameters such as solvent, temperature, reaction time, surfactant which may affect crystallinity and crystal defects of magnetite nanoparticles was negligible.

Furthermore, we carried out MRI experiments with the hollow and solid $Fe_3O_4$ nanorods. In order to quantitatively analyze the MRI relaxation properties, both

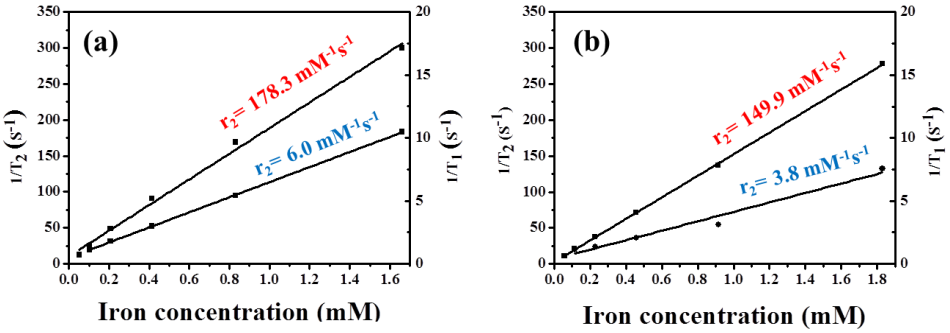


**Figure 8.** $T_1$ and $T_2$ relaxation rate ($1/T_1$, $1/T_2$) plotted against the Fe concentration for (a) hollow $Fe_3O_4$ and (b) solid $Fe_3O_4$ nanorods (0.47 T, 37 ℃)

**Table 2.** $r_1$ and $r_2$ relaxivities of hollow and solid $Fe_3O_4$ nanorods

| Sample | $r_1$ [$mM^{-1}s^{-1}$] | $r_2$ [$mM^{-1}s^{-1}$] | $r_2/r_1$ |
|---|---|---|---|
| Hollow $Fe_3O_4$ nanorods | 178.3 | 6.0 | 29.7 |
| Solid $Fe_3O_4$ nanorods | 149.9 | 3.8 | 39.4 |

longitudinal ($T_1$) and transverse ($T_2$) relaxation times of solid $Fe_3O_4$ and hollow $Fe_3O_4$ nanorods with different concentrations were measured using minispec spectroscopy (MQ20 NMR Analyzer) with a magnetic field of 0.47 T. **Figure 8** showed the relaxation rates $1/T_1$ and $1/T_2$ as a function of the iron concentration for the solid $Fe_3O_4$ and hollow $Fe_3O_4$ nanorods. The $r_1$ and $r_2$ are the longitudinal and transverse relaxivities, which represent the efficiency of the magnetite nanoparticles as a contrast agent shortens the proton relaxation times.[1] The longitudinal and transverse relaxivities ($r_1$ and $r_2$) of both solid $Fe_3O_4$ and hollow $Fe_3O_4$ nanorods were calculated, respectively. (**Table 2.)** The $r_1$ and $r_2$ relaxivites of hollow $Fe_3O_4$ nanorods were 6.0 $mM^{-1}s^{-1}$ and 178 $mM^{-1}s^{-1}$ respectively, whereas those of solid $Fe_3O_4$ nanorods were 3.8 $mM^{-1}s^{-1}$ and 149.9 $mM^{-1}s^{-1}$ respectively. The $r_2/r_1$ ratios were also calculated as 29.7 and 39.4. Such values suggested that they are more favorable as $T_2$ contrast agents due to their much larger $r_2$ value.

# Conclusion

Variable-shaped $Fe_3O_4$ nanoparticles were prepared through the phase transformation from β-FeOOH to $Fe_3O_4$ via polyol process. We successfully fabricated the shape of $Fe_3O_4$ nanoparticles to solid spheres, hollow rods and solid rods by controlling the experimental condition such as the presence of sodium acetate (NaOAc), the anion exchange of β-FeOOH. This synthetic method was easy and economical procedure without additional surfactants or reducing agents, had many advantages such as ease of scale up and size control by adjusting the size of precursor materials. We tried to understand the formation mechanism. The NaOAc would retain the rod shape of precursor (β-FeOOH) during phase transformation by providing the basicity and the ligands. Moreover, we suspected that chloride ions in Cl-FeOOH structure play a crucial role in the formation of hollow structure.

The magnetic properties of the $Fe_3O_4$ with different shapes were carried out at room temperature. Because of their large average grain size, the solid $Fe_3O_4$ spheres had the highest value of $M_s$. On the other hand, the $M_s$ of solid $Fe_3O_4$ rods was higher than that of hollow $Fe_3O_4$ rods due to spin-canting effect, although solid $Fe_3O_4$ rods had similar average gain size to that of hollow $Fe_3O_4$ rods. Regarding to the coercive force, solid spheres had the smallest $H_c$ because of their small shape anisotropy and the highest $M_s$. Meanwhile, the hollow $Fe_3O_4$ rods had the largest $H_c$ due to high shape, surface anisotropy and lower $M_s$. This result showed the shape-

dependent magnetic properties resulted from their different grain size, spin disorder, shape and surface anisotropy. It was possible to understand more accurate shape-dependent magnetic properties, because it wasn't needed to consider the other effect of experimental parameters such as temperature, concentration, solvent, reducing agent, surfactants etc., which could affect the crystallinity and crystal defects of nanoparticles.

Using their magnetic properties, we carried out MRI experiments with the hollow and solid $Fe_3O_4$ nanorods. It found that they could be good candidates as $T_2$-weighted MRI contrast agents due to their much larger $r_2$ value.

# Reference


1. J. Wan, W. Cai, X. Meng and E. Liu, *Chem. Commun.*, 2007, 5004-5006.
2. B. H. Kim, N. Lee, H. Kim, K. An, Y. I. Park, Y. Choi, K. Shin, Y. Lee, S. G. Kwon, H. B. Na, J. G. Park, T. Y. Ahn, Y. W. Kim, W. K. Moon, S. H. Choi and T. Hyeon, *J. Am. Chem. Soc.*, 2011, **133**, 12624-12631.
3. T.-J. Yoon, W. Lee, Y.-S. Oh and J.-K. Lee, *New J. Chem.*, 2003, **27**, 227-229.
4. C. T. Yavuz, J. T. Mayo, W. W. Yu, A. Prakash, J. C. Falkner, S. Yean, L. Cong, H. J. Shipley, A. Kan, M. Tomson, D. Natelson and V. L. Colvin, *Science*, 2006, **314**, 964-967.
5. M. Zhu and G. Diao, *J. Phys. Chem. C*, 2011, **115**, 18923-18934.
6. B. Luo, S. Xu, W.-F. Ma, W.-R. Wang, S.-L. Wang, J. Guo, W.-L. Yang, J.-H. Hu and C.-C. Wang, *J. Mater. Chem.*, 2010, **20**, 7107-7113.
7. S.-W. Cao, Y.-J. Zhu, M.-Y. Ma, L. Li and L. Zhang, *J. Phys. Chem. C*, 2008, **112**, 1851-1856.
8. D. Shi, H. S. Cho, Y. Chen, H. Xu, H. Gu, J. Lian, W. Wang, G. Liu, C. Huth, L. Wang, R. C. Ewing, S. Budko, G. M. Pauletti and Z. Dong, *Adv. Mater.*, 2009, **21**, 2170-2173.
9. W. Jiang, H. C. Yang, S. Y. Yang, H. E. Horng, J. C. Hung, Y. C. Chen and C.-Y. Hong, *J. Magn. Magn. Mater.*, 2004, **283**, 210-214.
10. N. R. Jana, Y. Chen and X. Peng, *Chem. Mater.*, 2004, **16**, 3931-3935.

11. S. Xuan, L. Hao, W. Jiang, X. Gong, Y. Hu and Z. Chen, *J. Magn. Magn. Mater.*, 2007, **308**, 210-213.

12. H. Deng, X. Li, Q. Peng, X. Wang, J. Chen and Y. Li, *Angew. Chem. Int. Ed.*, 2005, **44**, 2782-2785.

13. C. M. Cheng, Y. H. Wen, X. F. Xu and H. C. Gu, *J. Mater. Chem.*, 2009, **19**, 8782-8788.

14. J. Yue, X. Jiang and A. Yu, *J. Nanopart. Res.*, 2011, **13**, 3961-3974.

15. M. A. Blesa, M. Mijalchik, M. Villegas and G. Rigotti, *Reactivity of Solids*, 1986, **2**, 85-94.

16. Z. M. Peng, M. Z. Wu, Y. Xiong, J. Wang and Q. W. Chen, *Chem. Lett.*, 2005, **34**, 636-637.

17. W. Wu, X. Xiao, S. Zhang, J. Zhou, L. Fan, F. Ren and C. Jiang, *J. Phys. Chem. C*, 2010, **114**, 16092-16103.

18. S. Lian, E. Wang, L. Gao, Z. Kang, D. Wu, Y. Lan and L. Xu, *Solid State Commun.*, 2004, **132**, 375-378.

19. S. Lian, Z. Kang, E. Wang, M. Jiang, C. Hu and L. Xu, *Solid State Commun.*, 2003, **127**, 605-608.

20. G. Gao, X. Liu, R. Shi, K. Zhou, Y. Shi, R. Ma, E. Takayama-Muromachi and G. Qiu, *Crystal Growth & Design*, 2010, **10**, 2888-2894.

21. X. Wang, Z. Zhao, J. Qu, Z. Wang and J. Qiu, *Crystal Growth & Design*, 2010, **10**, 2863-2869.

22. P. Guardia, A. Labarta and X. Batlle, *J. Phys. Chem. C*, 2010, **115**, 390-396.

23. Y. Piao, J. Kim, H. B. Na, D. Kim, J. S. Baek, M. K. Ko, J. H. Lee, M. Shokouhimehr and T. Hyeon, *Nat Mater*, 2008, **7**, 242-247.

24. J. Cai, J. Liu, Z. Gao, A. Navrotsky and S. L. Suib, *Chem. Mater.*, 2001, **13**, 4595-4602.

25. S. Reguer, F. Mirambet, E. Dooryhee, J. L. Hodeau, P. Dillmann and P. Lagarde, *Corros. Sci.*, 2009, **51**, 2795-2802.

26. D. M. W. Douglas A. Skoog, F. James Holler, *Analytical chemistry : an introduction*, 1994.

27. S. Laurent, D. Forge, M. Port, A. Roch, C. Robic, L. V. Elst and R. N. Muller, *Chem. Rev.*, 2008, **108**, 2064-2110.

28. S. Gonielizalde, M. E. Garciaclavel and M. I. Tejedortejedor, *Reactivity of Solids*, 1987, **3**, 139-154.

29. H. D. Pedersen, D. Postma, R. Jakobsen and O. Larsen, *Geochim. Cosmochim. Acta*, 2005, **69**, 3967-3977.

30. A. G. B. Williams and M. M. Scherer, *Environmental Science & Technology*, 2004, **38**, 4782-4790.

31. U. S. R.M.Cornell, *The iron oxide; structure, properties, reactions, occurrence and uses*, 1996.

32. U. Schwertmann, *Plant and Soil*, 1991, **130**, 1-25.

33. K. Norén, J. S. Loring, J. R. Bargar and P. Persson, *J. Phys. Chem. C*, 2009, **113**, 7762-7771.

34. K. Stahl, K. Nielsen, J. Z. Jiang, B. Lebech, J. C. Hanson, P. Norby and J.

van Lanschot, *Corros. Sci.*, 2003, **45**, 2563-2575.

35. Y. C. Ling, G. M. Wang, J. Reddy, C. C. Wang, J. Z. Zhang and Y. Li, *Angewandte Chemie-International Edition*, 2012, **51**, 4074-4079.

36. B. Wang, J. S. Chen, H. B. Wu, Z. Wang and X. W. Lou, *J. Am. Chem. Soc.*, 2011, **133**, 17146-17148.

37. S. J. Yan, J. K. Tang, P. Liu, Q. Gao, G. Y. Hong and L. Zhen, *J. Appl. Phys.*, 2011, **109**.

38. S. H. Xuan, Y. X. J. Wang, J. C. Yu and K. C. F. Leung, *Chem. Mater.*, 2009, **21**, 5079-5087.

39. B. H. Kim, N. Lee, H. Kim, K. An, Y. I. Park, Y. Choi, K. Shin, Y. Lee, S. G. Kwon, H. B. Na, J.-G. Park, T.-Y. Ahn, Y.-W. Kim, W. K. Moon, S. H. Choi and T. Hyeon, *J. Am. Chem. Soc.*, 2011, **133**, 12624-12631.

40. S. Si, A. Kotal, T. K. Mandal, S. Giri, H. Nakamura and T. Kohara, *Chem. Mater.*, 2004, **16**, 3489-3496.

# 초 록

Akaganeite ($\beta$-FeOOH)를 이용하여 간단한 상 변화를 통해 magnetite ($Fe_3O_4$) 나노 입자의 형태 조절 합성이 가능했다. 속 찬 구형, 속 찬 막대형, 속 빈 막대형을 포함하는 다양한 형태의 $Fe_3O_4$ 나노 입자는 상 변화 반응에서의 sodium acetate (NaOAc)의 유무 또는 $\beta$-FeOOH의 음이온 교환을 조절하여 얻을 수 있었으며, 형태 조절된 나노 입자의 형성 메커니즘을 제안하였다. $\beta$-FeOOH로부터 $Fe_3O_4$로의 상 변화 시, NaOAc는 염기도를 높일 뿐만 아니라 acetate 음이온이 $\beta$-FeOOH 표면에 coordination하므로써 원래의 막대 모양을 유지할 수 있었다. 또한 $\beta$-FeOOH 구조 내부에 포함된 chloride 이온은 속 빈 구조체를 만드는데 결정적인 역할을 하는 것으로 생각되었다. 형태 의존 자기 특성은 상온에서 자성 측정 시스템을 이용하여 측정하였다. 형태에 관계없이 모두 페리 자성을 보였지만, 형태에 따라서 포화 자화도 ($M_s$)와 보자력 ($H_c$)에 차이가 있었다. 이는 형태에 따라 grain 크기, 스핀 무질서도, 모양 비등방성, 표면 비등방성 등이 달라지기 때문으로 이해할 수 있었다. 속 빈 막대 모양과 속 찬 막대 모양의 $Fe_3O_4$ 나노 입자의 경우 입자 크기와 grain 크기가 같으며, 나노 입자의 결정성과 defect에 영향을 줄 수 있는 온도, 용매, 반응 시간, surfactant와 같은 실험적 요소의 차이를 무시할 수

있기 때문에 더욱 정확한 형태 의존적 자기 특성의 비교가 가능했다. 또한 이들의 $r_1$ (longitudinal relaxivity)와 $r_2$ (transverse relaxivity)를 확인하였고, $T_2$ MRI 조영제로써의 응용 가능성을 확인하였다.

**주요어 :** Akaganeite (β-FeOOH), Magnetite ($Fe_3O_4$), 상 변화, 형태 조절 합성, 형태 의존적 자기 특성

**학 번 :** 2011-20309